

## Formation and Decay of Excited Hg<sub>2</sub> Molecules in Hg-N<sub>2</sub> Mixtures\*

R. A. Phaneuf,<sup>†</sup> J. Skonieczny,<sup>‡</sup> and L. Krause

*Department of Physics, University of Windsor, Windsor, Ontario, Canada*

(Received 22 August 1973)

The formation and decay of excited Hg<sub>2</sub> molecules formed in Hg-N<sub>2</sub> mixtures irradiated with 2537-Å Hg resonance radiation, has been investigated using methods of delayed coincidences. The vapor-gas mixtures contained in a quartz fluorescence cell were excited with pulses of light and the resulting decay spectra of the 3350- and 4850-Å molecular fluorescent bands were studied in relation to N<sub>2</sub> pressure. Both bands exhibited identical decay patterns which included a slower and a faster component, the latter being identical with that for the decay of the 2537-Å afterglow. Analysis of the decays indicates that the molecular <sup>3</sup>1<sub>u</sub> state (which is associated with the 3350-Å band) is formed first in a Hg(<sup>3</sup>P<sub>0</sub>) + Hg(<sup>1</sup>S<sub>0</sub>) + N<sub>2</sub> triple collision and the <sup>3</sup>0<sub>u</sub><sup>-</sup> state (associated with the 4850-Å band) is produced by subsequent molecular collisions of Hg<sub>2</sub>(<sup>3</sup>1<sub>u</sub>) with N<sub>2</sub>. The experiments yielded, in addition to the lower limit of the lifetime  $\tau(^30_u^-) > 4.5$  msec, the following total cross sections and rate constant:  $Q(^30_u^- \rightarrow ^31_u) = 5.5 \times 10^{-21}$  cm<sup>2</sup>;  $Q(^31_u \rightarrow ^30_u^-) \approx 3 \times 10^{-17}$  cm<sup>2</sup>;  $k(^3P_0 \rightarrow ^31_u) \approx 10^{-30}$  (cm<sup>-3</sup>)<sup>-2</sup> sec<sup>-1</sup>.

### I. INTRODUCTION

The fluorescent band spectra, which are observed when pure mercury vapor at high density is irradiated with the 2537-Å resonance line, have been the subject of several experimental studies.<sup>1</sup> This molecular fluorescence consists of two principal bands centered at 3350 and 4850 Å that are known to persist for milliseconds after extinguishing the exciting light. The afterglow was first observed by Phillips,<sup>2</sup> and later Rayleigh found evidence that both bands decayed simultaneously,<sup>3</sup> and that the metastable 6<sup>3</sup>P<sub>0</sub> atomic state was involved in their formation.<sup>4</sup> Franck and Grotrian<sup>5</sup> were the first to associate these bands with electronic excited states of the Hg<sub>2</sub> molecule. Mrozowski<sup>6,7</sup> subsequently suggested that it was the spontaneous decay of the A<sup>3</sup>0<sub>u</sub><sup>-</sup> and A<sup>3</sup>1<sub>u</sub> states of Hg<sub>2</sub> that was responsible for the 4850- and 3350-Å bands, respectively, and constructed potential curves based on this interpretation. More recent experiments by McCoubrey<sup>8</sup> have cast some doubt on this hypothesis. Observing that the two bands had a common persistence time and that the band intensity ratio  $I(4850 \text{ Å})/I(3350 \text{ Å})$  was proportional to the square of the mercury density, McCoubrey concluded that the 3350-Å band resulted from the decay of the A<sup>3</sup>0<sub>u</sub><sup>-</sup> state, while the presence of the 4850-Å band was due to collision-induced emission involving a triple collision between two (6<sup>1</sup>S<sub>0</sub>) ground-state mercury atoms and a <sup>3</sup>0<sub>u</sub><sup>-</sup> mercury molecule.

It is well known that these fluorescence bands also appear in mixtures of mercury and nitrogen at much lower mercury densities.<sup>6,9</sup> This is thought to be due to the fact that nitrogen is very efficient in quenching Hg(6<sup>3</sup>P<sub>1</sub>) atoms to the 6<sup>3</sup>P<sub>0</sub> metastable state.<sup>10</sup> Berberet and Clark<sup>11</sup> investi-

gated the intensity and decay rate of the 4850-Å band in the presence of nitrogen and concluded that an excited Hg<sub>2</sub> molecule was formed in a three-body collision of a Hg(<sup>3</sup>P<sub>0</sub>) atom, a Hg(<sup>1</sup>S<sub>0</sub>) atom, and an N<sub>2</sub> molecule. They further suggested that the decay of this Hg<sub>2</sub> molecule gave rise to the 4850-Å band. More recently, Penzes, Gunning, and Strausz<sup>12</sup> investigated the intensities of the two bands in the presence of nitrogen and other gases, and found that the intensity ratio  $I(4850 \text{ Å})/I(3350 \text{ Å})$  was proportional to the nitrogen density. They also observed that the bands appeared only when absorption of the 4047-Å line (6<sup>3</sup>P<sub>0</sub> → 7<sup>3</sup>S<sub>1</sub>) indicated the presence of Hg(<sup>3</sup>P<sub>0</sub>) metastable atoms. McAlduff, Drysdale, and LeRoy<sup>13</sup> observed that the intensity of the 4850-Å band was proportional to the product of the densities of Hg(<sup>1</sup>S<sub>0</sub>), Hg(<sup>3</sup>P<sub>0</sub>), and N<sub>2</sub>, and also to the intensity of the 2537-Å exciting radiation. They also found that the intensity ratio  $I(4850 \text{ Å})/I(3350 \text{ Å})$  was proportional to the nitrogen density. In order to explain these experimental results, both groups of investigators<sup>12,13</sup> were led to favor Mrozowski's original explanation for the origins of the bands. Stupavsky, Drake, and Krause<sup>14</sup> observed a well-resolved structure near 5500 Å in mixtures of mercury vapor and nitrogen, and suggested that the structure was due to transitions between vibrational levels of the excited Hg<sub>2</sub> molecule and its repulsive ground state. However, very recent results obtained by Vikis and LeRoy,<sup>15</sup> indicate the possibility that the observed structure might be due to excited HgCl molecules.

In the present investigation, the method of delayed coincidences has been used to monitor the persistence times of the 4850- and 3350-Å bands as well as of the long-lived 2537-Å afterglow<sup>10</sup> excited by pulses of resonance radiation in mix-

tures of mercury and nitrogen, in relation to nitrogen pressure. The nitrogen pressure was kept sufficiently high to keep to a minimum the effects of diffusion of metastable atoms and molecules to the cell walls<sup>10,16</sup> on the measured decay rates. It was hoped that the experiments would lead to definite conclusions as to the origins of the bands, and yield quantitative information about some of the radiative decay and collision rates involved. The latter are of particular importance because of recent interest in the  $^3O_u^- \rightarrow ^1\Sigma_g^+$  transition in Hg<sub>2</sub> as a possible vehicle for a molecular dissociation laser.<sup>17,18</sup>

## II. EXPERIMENTAL

The apparatus and experimental technique were similar to those used by Pitre, Hammond, and Krause<sup>10</sup> in their study of the long-lived 2537-Å afterglow in Hg-N<sub>2</sub> mixtures. Mercury resonance radiation emitted by a radio-frequency discharge lamp was mechanically chopped and focused into a fluorescence cell containing a mixture of mercury vapor and nitrogen at a fixed temperature. The fluorescence emitted perpendicularly to the direction of excitation was resolved by appropriate filters in series with a grating spectrometer, and was detected with a liquid-nitrogen-cooled Philips 56 TUV photomultiplier. A time-to-amplitude converter was used to measure the intervals between the exciting and fluorescent light pulses. The "start" pulses were obtained from an auxiliary photomultiplier onto whose photocathode was reflected a small portion of the exciting light beam; the output of the photomultiplier, which detected the fluorescence, provided the "stop" pulses. The resulting decay spectrum was accumulated in a 200 channel pulse-height analyzer and was recorded on punched paper tape.

The discharge lamp consisted of a cylindrical quartz tube which contained a drop of mercury and one end of which was housed in an oven. The temperature of the oven was kept at a constant temperature of 60 °C using a thermostatic circulator. The tube was placed within the tank coil of a 150-MHz oscillator. The precise control of mercury-vapor density in the lamp ensured high intensity and stability over long periods of time. The light from the lamp passed through a slit 15 mm long and 1 mm wide, and was focused onto a similar slit attached to a PAR model 222 variable-speed chopper. The latter was equipped with a special wheel containing four 2-cm wide tapered apertures. The rectangular light pulses were produced at a repetition rate of 200 pulses/sec, had rise and fall times of about 40 μsec and a duration of 750 μsec. Initially a Corning CS7-54

filter was placed in the incident light beam to prevent the mercury 6<sup>3</sup>P<sub>0</sub> metastable atoms from being excited to higher states. Subsequent experiments, however, showed that its removal had no influence on the measured decay rates and consequently its use was discontinued in order to enhance the fluorescent intensities.

The exciting light beam was focused in the rectangular corner between the entrance and observation windows of the fluorescence cell so that the path lengths of the exciting and observed fluorescent light in the vapor were approximately 5 mm. This dimension was chosen to effect a compromise between the reduction of radiation trapping and of diffusion of metastable atoms and molecules to the cell walls. The fluorescence cell was constructed of a 5-cm section of D-shaped GE type 151 nonfluorescing fused silica, and had plane windows of the same material sealed onto the ends. When illuminated with 2537-Å radiation, the fluorescence originating from the windows was too faint to be registered by the detection system. The cell was mounted in an oven whose temperature was maintained at (158.5 ± 1) °C, and was connected to a glass vacuum and gas-handling system by means of a greaseless magnetically operated stopcock which was located in the oven. The stopcock effectively prevented mercury vapor from condensing outside the cell and permitted rapid evacuation and admission of nitrogen. The cell was equipped with a side-arm reservoir which contained a drop of natural mercury of high purity and which was enclosed in a separate oven whose temperature was controlled by a thermostatic circulating bath. In this way, the density of the saturated mercury vapor in the cell could be maintained independently of the kinetic temperature of the mercury-nitrogen mixture. A set of Helmholtz coils centered at the cell canceled the earth's magnetic field in order to eliminate modulation of the decay in experiments with pure mercury vapor.<sup>19</sup> The fluorescence cell as well as the vacuum and gas-handling system were baked out under vacuum for considerable periods of time. Nitrogen pressure was measured with a mercury manometer.

The fluorescent light from the vapor-gas mixture was resolved using a Perkin-Elmer model 112 scanning spectrometer equipped with a Jarell-Ash replica grating ruled at 1180 grooves/mm and blazed at 3000 Å in the first order. When detecting the molecular fluorescence bands, a Corning CG 774 (Pyrex) filter was placed in series with the spectrometer to eliminate the 2537-Å stray light scattered in the instrument. Because of the limited scanning range of the spectrometer, it was convenient to monitor the 2537-Å afterglow

in the second order of the grating with a Corion 2537-Å interference filter (bandwidth of 150 Å) used in series with the spectrometer to eliminate the contribution to the observed signal from the overlapping 4850-Å band fluorescence.

The voltage pulses from the reference photomultiplier were amplified and delayed until the exciting pulse had fully died away, and were appropriately shaped before being applied to the "start" terminal of the Ortec model 457S time-to-amplitude (TAC) converter. The pulse-height analyzer was calibrated using an Ad-Yu model 802E delay line with an accuracy better than 2%. The linearity of the TAC multichannel analyzer system was verified over the 200 channels to within one channel.

The exponential decay spectra were analyzed on an IBM 360-65 computer using a modified FRANTIC<sup>20</sup> program in which the data were corrected for "pile up," or discrimination against the detection of longer-lived excited species.<sup>21</sup> In all the experiments, the sensitivity of the detection system was adjusted so that not more than one stop pulse was obtained for every ten exciting pulses. Under these conditions the corrections amounted to only a few percent.

### III. RESULTS

To decrease the imprisonment of resonance radiation in the vapor while maintaining acceptable intensities of the molecular fluorescence bands, the mercury reservoir in the fluorescence cell was kept at a constant temperature of  $(60 \pm 0.1)^\circ\text{C}$  during all the experimental runs. This corresponded to a saturated mercury vapor density of  $7.7 \times 10^{14} \text{ cm}^{-3}$ . The experimentally measured effective decay time of the imprisoned 2537-Å radiation in pure mercury under these conditions was  $(10 \pm 1) \mu\text{sec}$ . This should be compared with a value of  $9.7 \mu\text{sec}$  which was calculated using the experimentally verified relation given by Holstein, Alpert, and McCoubrey<sup>22</sup> assuming an optical path of 0.5 cm.

To investigate the decay spectra of the two molecular fluorescence bands, the spectrometer was set at either 5000 or 3400 Å. The use of 0.75-mm-slit widths resulted in a half-bandwidth of approximately 33 Å. The decay spectra of both bands as well as of the 2537-Å afterglow were obtained at various nitrogen pressures in the range 35–760 torr. The influence on the decay rates of diffusion of metastable species to the cell walls<sup>10,16</sup> or out of the region of observation<sup>23</sup> was ascertained from additional data taken at lower pressures. Corrections to the decay rates, which were determined in the manner employed by Pitre, Ham-

mond, and Krause,<sup>10</sup> amounted to 10% for the molecular fluorescence at 35 torr of  $\text{N}_2$  (decreasing rapidly with increasing pressure), and were insignificant for the 2537-Å afterglow.

Considerable care was taken to reduce the effects of impurities on the measured decay rates. The Matheson research-grade nitrogen which was used in the experiments was specified to contain less than 1 ppm of potential impurities which are known to quench either  $\text{Hg}(^3P_0)$  or  $\text{Hg}(^3P_1)$  atoms to the ground state. In order to remove any impurities that might be adsorbed on the walls of the fluorescence cell, the latter was evacuated and baked several times during the course of the experiments. Measurements were carried out always with decreasing  $\text{N}_2$  pressure and the reproducibility of the data was verified by returning several times to higher pressures of nitrogen.

A typical decay spectrum for the 4850-Å band is shown in Fig. 1. Each such spectrum required an accumulation time of approximately 2 h. The distinct presence of two exponential components, one of which had a negative amplitude, was verified by computer analysis, the result being indicated by the solid curve. The existence of this additional component was observed in the decay spectra of both the 4850- and 3350-Å molecular bands. Similar decay curves have been obtained by McCoubrey<sup>8</sup> in experiments with pure mercury vapor. In the present investigation, the amplitude of the shorter-lived negative component relative to that of longer-lived decay was found to be larger in case of the 4850-Å band at all nitrogen pressures. In addition, at any given nitrogen pressure, the decay rates for both molecular bands were found to be equal within experimental

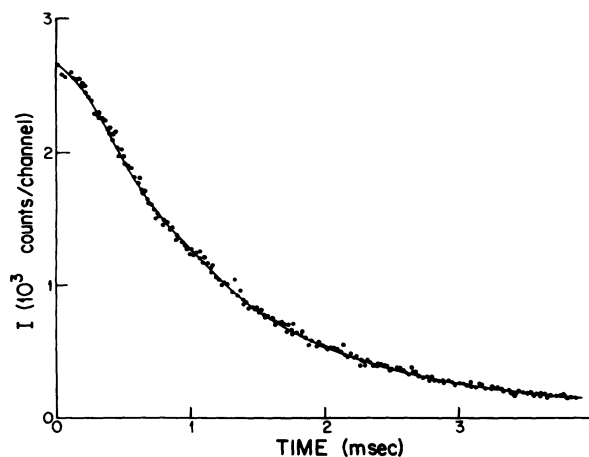


FIG. 1. Typical decay spectrum of the 4850-Å molecular band in the presence of 199 torr of  $\text{N}_2$ . The solid curve represents a least-squares fit of the experimental data.

error. The fact that, in pure mercury vapor, the two molecular fluorescence bands decay with a common persistence time, has been observed by several authors.<sup>3,8,24</sup> The variation of the longer-lived decay constant  $\Gamma_b$  with N<sub>2</sub> pressure is shown in Fig. 2. Each experimental point represents the average of the values obtained for both fluorescent bands at a particular pressure.

Figure 3 shows the variation with N<sub>2</sub> pressure of the decay constant for the 2537-Å afterglow which arises from  $^3P_0 - ^3P_1$  excitation transfer induced in collisions between Hg( $6^3P_0$ ) atoms and N<sub>2</sub> molecules.<sup>10</sup> A single exponential decay was observed at all N<sub>2</sub> pressures. It also appeared that, at each N<sub>2</sub> pressure, the measured decay constant for the 2537-Å afterglow was equal within experimental error to the decay constant for the shorter-lived component of negative amplitude, which was observed in the decay of the molecular fluorescence. As will be shown later, this should be expected if  $6^3P_0$  metastable mercury atoms participate in the formation of the excited Hg<sub>2</sub> molecules. The dashed curve in Fig. 4 represents the results of Pitre, Hammond, and Krause<sup>10</sup> obtained at room temperature and at a mercury-vapor density of  $2 \times 10^{11}$  cm<sup>-3</sup>, at which the imprisonment of resonance radiation and the formation of excited Hg<sub>2</sub> molecules may be neglected.

#### IV. INTERPRETATION AND DISCUSSION OF RESULTS

##### A. A Model for Production of Hg<sub>2</sub> Molecules

The fact that both the 4850- and 3350-Å molecular fluorescence bands decay simultaneously, suggests the existence of a common reservoir

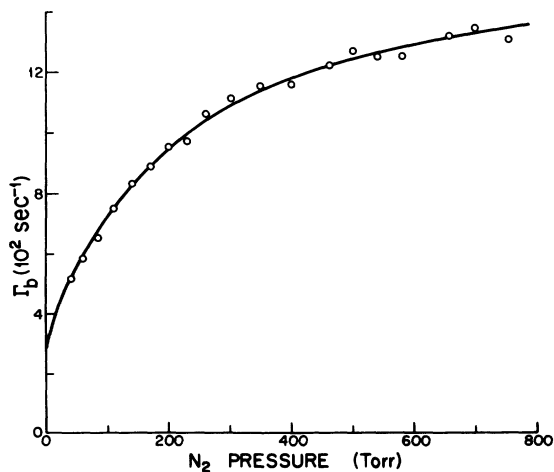


FIG. 2. Variation of the decay rate  $\Gamma_b$  with N<sub>2</sub> pressure at a mercury-vapor density of  $7.7 \times 10^{14}$  cm<sup>-3</sup> and assuming  $\Gamma_3 = 8.54 \times 10^6$  sec<sup>-1</sup> in the least-squares fit of Eq. (27) to the experimental points.

of excitation energy, which may be regarded as the source of both  $^3P_1$  and  $^3P_0$  molecules. The further fact that two decay constants are associated with the decay of the molecular fluorescence, indicates the existence of two separate reservoirs connected with each other. That the decay rate of negative amplitude, associated with the molecular bands, is numerically equal to that observed in the decay of the 2537-Å afterglow, leads to the conclusion that the metastable  $^3P_0$  state may constitute the primary reservoir. This is likely so because, as will be shown later, collisional excitation transfer between Hg( $^3P_0$ ) and Hg( $^3P_1$ )<sup>10</sup> causes the populations of both states to decay with the same time constants. Since the radiative lifetime of the  $6^3P_1$  state is relatively short, the metastable  $6^3P_0$  state might reasonably be expected to be the primary source of molecular excitation. This has been confirmed experimentally by Penzes, Gunning, and Strausz,<sup>12</sup> who were able to detect the bands only in the presence of Hg( $6^3P_0$ ) atoms.

The mechanism suggested by McAlduff, Drysdale, and LeRoy<sup>13</sup> and by Penzes, Gunning, and Strausz,<sup>12</sup> to account for the formation and decay of the excited molecular states in the presence of N<sub>2</sub>, which was based on Mrozowski's original proposal,<sup>6,7</sup> will be shown consistent with the results of the present investigation. The relevant potential curves for the Hg<sub>2</sub> molecule as given by

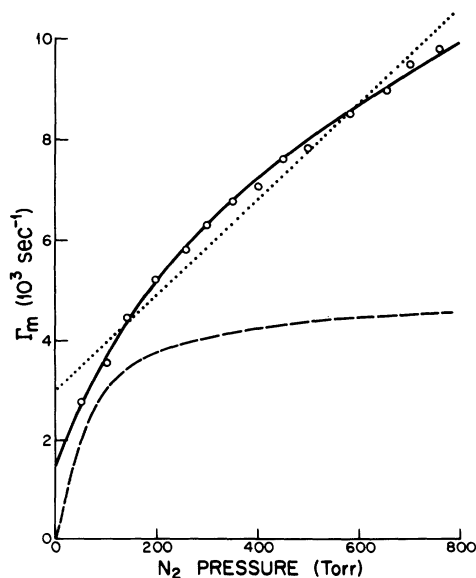
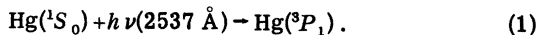
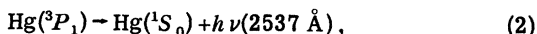


FIG. 3. Variation of the decay rate  $\Gamma_m$  with N<sub>2</sub> pressure at a mercury-vapor density  $N(\text{Hg}) = 7.7 \times 10^{14}$  cm<sup>-3</sup>. Dashed line, results of Pitre *et al.* with  $N(\text{Hg}) = 2 \times 10^{11}$  cm<sup>-3</sup>; solid line, fit of Eq. (19) to the experimental data assuming  $\Gamma_2 = 8.54 \times 10^6$  sec<sup>-1</sup>; dotted line, fit of Eq. (19) using  $\Gamma_2$  as given by Eq. (32).

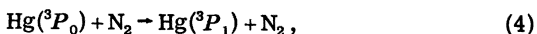
Mrozowski,<sup>7</sup> are shown in Fig. 4. The first step in the process leading to the emission of molecular fluorescence is the absorption of mercury resonance radiation by ground-state  $\text{Hg}(6^1S_0)$  atoms:



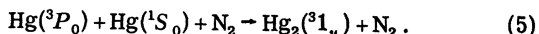
Assuming negligible quenching to the ground state,<sup>10</sup> the  $\text{Hg}(^3P_1)$  population then decays by one of two processes:



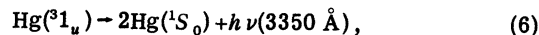
The metastable  $\text{Hg}(^3P_0)$  atoms can either be transferred back to the  $^3P_1$  state,



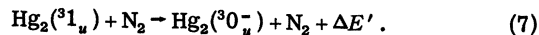
or they can combine with the ground-state mercury atoms to form  $\text{Hg}_2$  molecules in three-body collisions:



The formation of  $\text{Hg}_2$  molecules in the  $^31_u$  state as the result of such a collision has been explained by Mrozowski.<sup>6</sup> The  $^30_u^-$  and  $^31_u$  molecular states merge into a single  $^3\Sigma_u^+$  state at moderate internuclear distances. This energy region lies below the dissociation limit of the  $^30_u^-$  state, so that a combination  $\text{Hg}(^3P_0) + \text{Hg}(^1S_0)$  should populate both states equally. Since there can be no dissociation along the  $^31_u$  potential curve, collisional stabilization should occur more readily in this state and the population of  $^31_u$  molecules could then be assumed to decay either by spontaneous emission, giving rise to the band at 3350 Å,

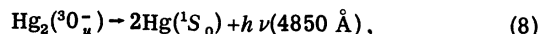


or by collisional transfer to the  $^30_u^-$  state,

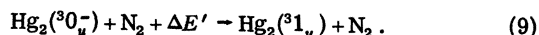


The latter process, which is the molecular analog of the  $6^3P_1 - 6^3P_0$  transfer, should also be very efficient because of the fairly close match between the energy difference  $\Delta E'$  and the spacing of vibrational levels in  $\text{N}_2$ .<sup>6</sup>

The  $^30_u^-$  molecules can decay either by spontaneous emission, giving rise to the 4850-Å band,



or can be transferred back to the  $^31_u$  state in collisions with  $\text{N}_2$  molecules,



The radiative decay of the  $^30_u^-$  state to the  $^1\Sigma_g^+$  ground state is forbidden, but at small internuclear distances, where the  $^30_u^-$  and  $^31_u$  states merge into a  $^3\Sigma_u^+$  state, the transition probability can be as high as  $10^7 \text{ sec}^{-1}$ . This corresponds to a change from Hund's coupling case (c) to case (a) resulting from an interaction between the atoms which causes vectors  $\vec{L}$  and  $\vec{S}$  to precess independently about the internuclear axis.<sup>25</sup> Because the vibrating metastable molecules trapped in the  $^30_u^-$  state radiate only at the time of closest approach of the two atoms, the 4850-Å band is emitted mainly by molecules with high vibrational energies. The observed lifetime of the order of milliseconds represents an average which depends on the mean vibrational energy of the  $\text{Hg}_2$  gas, and thus on the temperature. For the  $^31_u$  state, however, a constant transition probability comparable to that of the atomic  $^3P_1$  state should be expected over the entire range of internuclear distances.

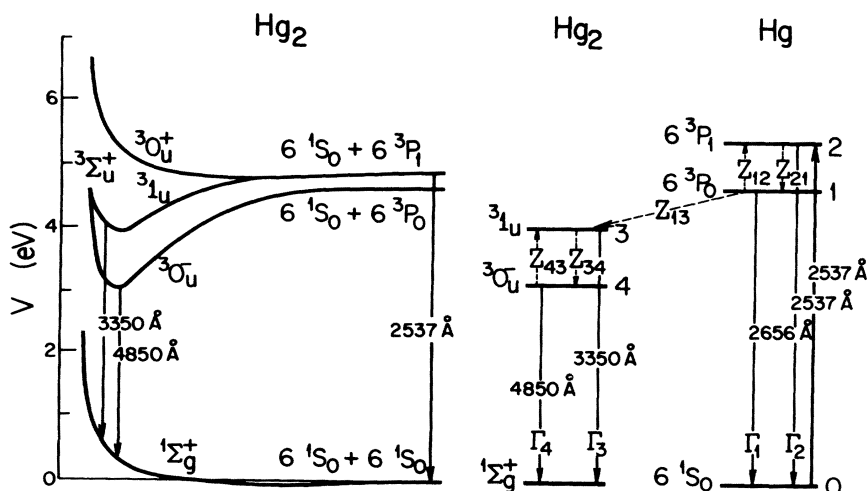


FIG. 4. Schematic diagram of atomic and molecular levels and processes involved in the sensitized fluorescence of  $\text{Hg}_2$  molecules. The molecular potential energy curves follow the scheme of Mrozowski.

### B. Rate Equations for the Population and Decay of Atomic and Molecular States

The appropriate atomic and molecular levels of mercury as well as the various radiative and collisional processes which have been discussed, are shown schematically in Fig. 4. Quenching of excited atomic and molecular species to the ground state and collisional dissociation of stabilized Hg<sub>2</sub> molecules are considered to be relatively unimportant and are not included. The corresponding rate equations for the populations  $n_i$  of the various states become

$$\dot{n}_1 = -(\Gamma_1 + Z_{12} + Z_{13})n_1 + Z_{21}n_2, \quad (10)$$

$$\dot{n}_2 = -(\Gamma_2 + Z_{21})n_2 + Z_{12}n_1, \quad (11)$$

$$\dot{n}_3 = -(\Gamma_3 + Z_{34})n_3 + Z_{43}n_4 + Z_{13}n_1, \quad (12)$$

$$\dot{n}_4 = -(\Gamma_4 + Z_{43})n_4 + Z_{34}n_3, \quad (13)$$

where the subscripts 1, 2, 3, 4 denote the states  ${}^3P_0$ ,  ${}^3P_1$ ,  ${}^3I_u$ , and  ${}^3O_u^-$ , respectively,  $Z_{ij}$  represents the frequency of collisions per excited atom or molecule in state  $i$  resulting in a transfer to state  $j$ , and  $\Gamma_i$  is the decay constant for radiative decay of state  $i$  ( $\Gamma_i = 1/\tau_i$ , where  $\tau_i$  is the corresponding lifetime).

#### 1. Solutions for $n_1$ ( ${}^3P_0$ ) and $n_2$ ( ${}^3P_1$ )

The coupled differential Eqs. (10) and (11) may be separated and yield the following two second-order equations:

$$\ddot{n}_1 + (R_1 + R_2)\dot{n}_1 + (R_1R_2 - Z_{21}Z_{12})n_1 = 0, \quad (14)$$

$$\ddot{n}_2 + (R_1 + R_2)\dot{n}_2 + (R_1R_2 - Z_{21}Z_{12})n_2 = 0, \quad (15)$$

where

$$R_1 \equiv \Gamma_1 + Z_{12} + Z_{13} \text{ and } R_2 \equiv \Gamma_2 + Z_{21}. \quad (16)$$

It may be seen that the populations  $n_1$  and  $n_2$  satisfy exactly the same differential equation. The solutions are

$$n_1 = Ae^{-\Gamma_m t} + Be^{-\Gamma'_m t}, \quad (17)$$

$$n_2 = A'e^{-\Gamma_m t} + B'e^{-\Gamma'_m t}, \quad (18)$$

where

$$\Gamma_m = \frac{1}{2}(R_1 + R_2) - \frac{1}{2}[(R_2 - R_1)^2 + 4Z_{21}Z_{12}]^{1/2}, \quad (19)$$

and

$$\Gamma'_m = \frac{1}{2}(R_1 + R_2) + \frac{1}{2}[(R_2 - R_1)^2 + 4Z_{21}Z_{12}]^{1/2}. \quad (20)$$

$\Gamma'_m$  represents the short-lived component and  $\Gamma_m$  the longer-lived component of the decay. In the range of observation times used in the present investigation, only the long-lived component  $\Gamma_m$  was detected, since  $\Gamma'_m$  is of the order of  $10^7 \text{ sec}^{-1}$

or larger.<sup>10</sup> It has thus been assumed that the  ${}^3P_0$  atoms decay with time constant  $\Gamma_m$  and

$$n_1 \approx Ae^{-\Gamma_m t}. \quad (21)$$

As predicted by Eqs. (17) and (18),  $\Gamma_m$  should correspond exactly to the decay constant associated with the 2537-Å afterglow.

#### 2. Solutions for $n_3$ ( ${}^3I_u$ ) and $n_4$ ( ${}^3O_u^-$ )

The substitution of the solution for  $n_1$  from Eq. (21) and the separation of Eqs. (12) and (13) results in the following inhomogeneous differential equations for  $n_3$  and  $n_4$ :

$$\ddot{n}_3 + (R_3 + R_4)\dot{n}_3 + (R_3R_4 - Z_{43}Z_{34})n_3 = Z_{13}A(R_4 - \Gamma_m)e^{-\Gamma_m t}, \quad (22)$$

$$\ddot{n}_4 + (R_3 + R_4)\dot{n}_4 + (R_3R_4 - Z_{43}Z_{34})n_4 = Z_{13}Ae^{-\Gamma_m t}, \quad (23)$$

where

$$R_3 \equiv \Gamma_3 + Z_{34}, \quad R_4 \equiv \Gamma_4 + Z_{43}. \quad (24)$$

It may be seen that the populations  $n_3$  and  $n_4$  obey differential equations which differ only in the amplitude of the right-hand-side term. The solutions are

$$n_3 = \alpha e^{-\Gamma_b t} + \beta e^{-\Gamma'_b t} + \delta e^{-\Gamma_m t}, \quad (25)$$

$$n_4 = \alpha' e^{-\Gamma_b t} + \beta' e^{-\Gamma'_b t} + \delta' e^{-\Gamma_m t}, \quad (26)$$

where

$$\Gamma_b = \frac{1}{2}(R_3 + R_4) - \frac{1}{2}[(R_3 - R_4)^2 + 4Z_{43}Z_{34}]^{1/2}, \quad (27)$$

and

$$\Gamma'_b = \frac{1}{2}(R_3 + R_4) + \frac{1}{2}[(R_3 - R_4)^2 + 4Z_{43}Z_{34}]^{1/2}. \quad (28)$$

Equations (25) and (26) indicate that both the  ${}^3I_u$  and  ${}^3O_u^-$  molecular states should decay with the same time constants. This has been confirmed experimentally as has the presence of the rate constant  $\Gamma_m$ , which is associated with the decay of the  ${}^3P_0$  metastable state and of the 2537-Å afterglow.

Since the radiative decay rate  $\Gamma_3$  of the  ${}^3I_u$  state is of the order of  $10^7 \text{ sec}^{-1}$ , it can be shown from Eq. (28) that in our range of observation times, the short-lived component  $\Gamma'_b$  which is at least as large as  $\Gamma_3$ , is not observable. Consequently,

$$n_3 \approx \alpha e^{-\Gamma_b t} + \delta e^{-\Gamma_m t}, \quad (29)$$

$$n_4 \approx \alpha' e^{-\Gamma_b t} + \delta' e^{-\Gamma_m t}. \quad (30)$$

### C. Analysis of Experimental Results

In order to further test the compatibility of the proposed model with the experimental results, Eq. (27) which predicts the variation of the decay

rate  $\Gamma_b$  with  $N_2$  pressure, was fitted to the experimental data by a least-squares analysis. In the analysis,  $\Gamma_3$  was initially put equal to  $\Gamma_2$  ( $8.54 \times 10^6 \text{ sec}^{-1}$ ). The resulting values of  $Z_{34}$ ,  $Z_{43}$ , and  $\Gamma_4$  are listed in Table I together with their standard deviations. The curve in Fig. 2 represents Eq. (27) including these parameters. The fit to the experimental data is very satisfactory. To test the sensitivity of the various parameters to  $\Gamma_3$ , the latter was assigned various values ranging from  $3 \times 10^6 \text{ sec}^{-1}$  to  $3 \times 10^7 \text{ sec}^{-1}$ , and the least-squares analysis was repeated for each value of  $\Gamma_3$  to obtain the corresponding magnitudes of the other three parameters. The results for the two extreme cases are also listed in Table I. Over this range of  $\Gamma_3$ , the standard deviation of the fit was not significantly altered, so that no inference can be drawn from these data as to the precise magnitude of  $\Gamma_3$ . It may be seen from Table I that, although  $\Gamma_3$  is changed by a factor of 10, the values obtained for  $\Gamma_4$  and  $Z_{43}$  are not altered by more than 1%; the same is not true for  $Z_{34}$  whose magnitude also changes by a factor of 10. Consequently we conclude that the values obtained for  $\Gamma_4$  and  $Z_{43}$  are not affected by the uncertainty in  $\Gamma_3$ .

An attempt was made to measure  $\Gamma_3$  by irradiating pure mercury vapor at very high density with 3371-Å radiation from a pulsed nitrogen laser, with the hope of optically exciting the  $\text{Hg}_2(^3\text{I}_u^-)$  state. The present design of the apparatus limited the maximal mercury pressure to about 1 atm and the temperature to about 400°C. Under these conditions, no fluorescence from the vapor could be detected. Lennuier and Crenn<sup>26</sup> irradiated pure mercury vapor at 600 torr and 380°C with light of wavelengths longer than 2537 Å and observed the 3350-Å fluorescent band, but found that, when exciting with wavelengths above 3300 Å, the resulting fluorescence was very faint. That no appreciable absorption was obtained in the present experiment is probably due to the relatively steep slope of the repulsive  $\text{Hg}_2(^1\Sigma_g^+)$  potential-energy curve in the transition region and to the narrow bandwidth of the exciting radiation.

It should also be kept in mind that the effective

values  $\Gamma_3$  and  $\Gamma_4$  yielded by the experiment, include collisional depopulation processes which do not involve  $N_2$  molecules. Consequently, the value obtained for  $\Gamma_4$  should be regarded as an upper limit of the decay constant for the radiative decay of the  $^3\text{O}_u^-$  state.

The interpretation of the variation of the decay constant  $\Gamma_m$  observed in the 2537-Å afterglow with  $N_2$  pressure, shown in Fig. 3, is complicated by imprisonment of the 2537-Å radiation in the vapor and by collision broadening of the absorption line which has the effect of reducing the imprisonment time as the  $N_2$  pressure is increased. To obtain an estimate for the variation of the imprisonment time with  $N_2$  pressure, the theory of Holstein<sup>27</sup> was applied in a manner analogous to that outlined by Matland.<sup>28</sup> According to the theory, pressure broadening of the mercury absorption line has the effect of reducing the imprisonment time  $T_i$  observed in the absence of  $N_2$ , according to the relation

$$1/T_i' \approx 1/T_i + \Delta\beta_p, \quad (31)$$

where  $T_i'$  is the imprisonment time corrected for pressure broadening and the quantity  $\Delta\beta_p$  depends linearly on  $N_2$  pressure. Using the broadening cross section quoted by Mitchell and Zeman-sky,<sup>29</sup> the calculation yielded the following expression for the behavior of the effective decay rate  $\Gamma_2$  in relation to  $N_2$  pressure  $P$  (in torr):

$$\Gamma_2 \approx (10^5 + 1.04 \times 10^4 P) \text{ sec}^{-1}, \quad (32)$$

where  $10^5 \text{ sec}^{-1}$  is the experimentally measured decay constant in pure mercury vapor at a density of  $7.7 \times 10^{14} \text{ cm}^{-3}$ . The expression for  $\Gamma_2$  was substituted into Eq. (19) and a least-squares fit was made of this equation to the experimental data for the decay constant  $\Gamma_m$  of the 2537-Å afterglow. In the analysis, the principle of detailed balance was invoked in order to express the rate  $Z_{21}$  in terms of  $Z_{12}$ , thus eliminating one parameter (the predicted ratio had been verified experimentally by Pitre, Hammond, and Krause<sup>10</sup>). The result of the fit is shown as a dotted line in Fig. 3. It was found that a linear dependence of  $\Gamma_m$  on  $N_2$  pressure was predicted for all values

TABLE I. Results of least-squares analyses using Eq. (27) and data points in Fig. 2.  $N$  denotes  $N_2$  density.

Assumed $\Gamma_3(\text{sec}^{-1})$	Parameters yielded by least-squares analysis				Standard deviation in $\Gamma_b(\text{sec}^{-1})$
	$\Gamma_4(\text{sec}^{-1})$	$Z_{43}(\text{sec}^{-1})$	$Z_{34}(\text{sec}^{-1})$		
$8.54 \times 10^6$	$223 \pm 38$	$(3.24 \pm 0.38) \times 10^{-16} (N)$	$(1.98 \pm 0.22) \times 10^{-12} (N)$	22.2	
$3.00 \times 10^6$	$223 \pm 38$	$(3.24 \pm 0.37) \times 10^{-16} (N)$	$(6.95 \pm 0.77) \times 10^{-13} (N)$	22.2	
$3.00 \times 10^7$	$222 \pm 40$	$(3.24 \pm 0.39) \times 10^{-16} (N)$	$(7.05 \pm 0.82) \times 10^{-12} (N)$	22.2	

TABLE II. Results of least-squares analyses using Eq. (19) and data points in Fig. 3. *P* denotes the pressure and *N* the density of N<sub>2</sub>.

Parameters yielded by least-squares analysis					
Assumed Γ <sub>2</sub> (sec <sup>-1</sup> )	Γ <sub>1</sub> (sec <sup>-1</sup> )	Z <sub>13</sub> (sec <sup>-1</sup> )	Z <sub>12</sub> (sec <sup>-1</sup> )	Z <sub>21</sub> (sec <sup>-1</sup> ) from Z <sub>12</sub> by detailed balancing	Standard deviation in Γ <sub>m</sub> (sec <sup>-1</sup> )
10 <sup>5</sup> + 1.04 × 10 <sup>4</sup> ( <i>P</i> )	3008 ± 602	(8.7 ± 181) × 10 <sup>-16</sup> ( <i>N</i> )	(1.5 ± 39.5) × 10 <sup>-15</sup> ( <i>N</i> )	(1.8 ± 47.6) × 10 <sup>-12</sup> ( <i>N</i> )	406
8.54 × 10 <sup>6</sup>	1527 ± 212	(6.94 ± 0.69) × 10 <sup>-16</sup> ( <i>N</i> )	(1.02 ± 0.14) × 10 <sup>-15</sup> ( <i>N</i> )	(1.23 ± 0.17) × 10 <sup>-12</sup> ( <i>N</i> )	117

of the parameters, contrary to the experimental observations. The observed behavior of the experimental data can, however, be very well represented by Eq. (19) if Γ<sub>2</sub> is assumed to be equal to the "natural" radiative decay constant for the Hg(6<sup>3</sup>P<sub>1</sub>) state (8.54 × 10<sup>6</sup> sec<sup>-1</sup>). The appropriate least-squares fit is indicated by the solid curve in Fig. 3 and the parameters which are obtained using the two procedures for assigning Γ<sub>2</sub> are listed in Table II. In addition to the radiative decay of the Hg(6<sup>3</sup>P<sub>0</sub>) state, the experimentally determined Γ<sub>1</sub> includes all collisional depopulation processes which do not involve N<sub>2</sub> molecules. Since the radiative decay rate of the Hg(6<sup>3</sup>P<sub>0</sub>) state has been shown to be about 2 sec,<sup>30</sup> collisions with ground-state mercury atoms ought to make

the largest contribution to Γ<sub>1</sub>. Because of the uncertainties which arise as the result of radiation trapping and collision broadening of the resonance line, the parameters obtained in the analysis of the 2537-Å afterglow are considered accurate only within order of magnitude.

The lifetime τ<sub>4</sub>, rate constant k<sub>13</sub>, and cross sections for the various processes of excitation transfer, resulting from the experiments, are listed in Table III. The cross sections Q<sub>ij</sub> have been calculated from the relation

$$Z_{ij} = Nv_r Q_{ij}, \quad (33)$$

where *N* is the density of N<sub>2</sub> molecules and *v<sub>r</sub>* is the mean relative speed of the colliding partners.

TABLE III. Radiative and collisional parameters pertinent to Hg<sub>2</sub> fluorescence.

Source	τ <sub>4</sub> ( <sup>3</sup> O <sub>u</sub> <sup>-</sup> ) (msec)	Q <sub>43</sub> (cm <sup>2</sup> )	Q <sub>34</sub> (cm <sup>2</sup> )	k <sub>13</sub> [(cm <sup>-3</sup> ) <sup>-2</sup> sec <sup>-1</sup> ]	Q <sub>12</sub> (cm <sup>2</sup> )	Q <sub>21</sub> (cm <sup>2</sup> )	Q <sub>1</sub> (Hg-Hg) (cm <sup>2</sup> )
This investigation <sup>a</sup>	> 4.5	5.5 × 10 <sup>-21</sup> ± 15%	~3 × 10 <sup>-17</sup>	~10 <sup>-30</sup>	~10 <sup>-20</sup>	~10 <sup>-17</sup>	~10 <sup>-16</sup>
Deech <i>et al.</i> (Ref. 25) <sup>b</sup>						7.2 × 10 <sup>-17</sup>	
Barrat <i>et al.</i> (Ref. 32) <sup>b</sup>						< 10 <sup>-16</sup>	
Matland (Ref. 29) <sup>c</sup>						6.2 × 10 <sup>-17</sup>	
Pitre <i>et al.</i> (Ref. 10) <sup>b</sup>					4.18 × 10 <sup>-20</sup>		
Callear and Williams (Ref. 33) <sup>b</sup>							~2.4 × 10 <sup>-15</sup>
McCoubrey (Ref. 8) <sup>d</sup>	50			10 <sup>-30</sup> e			
McAlduff <i>et al.</i> (Ref. 13 and 34) <sup>b</sup>			< 4 × 10 <sup>-17</sup>	1330 × 10 <sup>-30</sup>			
Penzes <i>et al.</i> (Ref. 12) <sup>b</sup>			~2.6 × 10 <sup>-15</sup>	3.06 × 10 <sup>-30</sup>			
Campbell <i>et al.</i> (Ref. 35) <sup>b</sup>				10.5 × 10 <sup>-30</sup>			

<sup>a</sup> Result at 432 °K.<sup>b</sup> Result at 296 °K.<sup>c</sup> Result at 420 °K.<sup>d</sup> Result at 473 °K.<sup>e</sup> Result obtained with Hg instead of N<sub>2</sub> as third body.

Some results obtained by other authors have been included for comparison. In most cases where other measurements have been reported, there is agreement within order of magnitude or better. The cross sections  $Q_{34}$  and  $Q_{43}$  for the  $^3\text{I}_u \rightarrow ^3\text{O}_u^-$  molecular transitions are similar in magnitude to  $Q_{21}$  and  $Q_{12}$  for the analogous atomic transitions  $^3\text{P}_1 \rightarrow ^3\text{P}_0$ . Because of radiation trapping, the latter values are not nearly as accurate as those determined previously,<sup>10,31</sup> but are of the correct order of magnitude.  $Q_1$  (Hg-Hg), the total cross section for depopulation of the Hg( $6^3\text{P}_0$ ) state by collisions with ground-state mercury atoms, was calculated assuming that the decay constant  $\Gamma_1$  was associated with this process.

In addition to the quantitative information given in Table III, the results of this investigation provide evidence for the mechanism by which the molecular states  $^3\text{I}_u$  and  $^3\text{O}_u^-$  are formed and the crucial steps of which are represented by Eqs. (5) and (7). The initial formation of  $^3\text{I}_u$  molecules (rather than  $^3\text{O}_u^-$  molecules) in three-body collisions, which is an essential ingredient of the

model, may be deduced from the variation of the intensity ratio  $I(4850 \text{ \AA})/I(3350 \text{ \AA})$  with  $\text{N}_2$  pressure. Setting  $\dot{n}_4 = 0$  in Eq. (13), yields

$$\frac{I(4850 \text{ \AA})}{I(3350 \text{ \AA})} = \frac{n_4 \Gamma_4}{n_3 \Gamma_3} = \frac{Z_{34} \Gamma_4}{\Gamma_3 (Z_{43} + \Gamma_4)}. \quad (34)$$

Assuming  $\Gamma_3 = \Gamma_2 = 8.54 \times 10^6 \text{ sec}^{-1}$  and substituting values for  $\Gamma_4$ ,  $Z_{34}$ , and  $Z_{43}$  from Table I in Eq. (34), results in a rapid increase of  $I(4850 \text{ \AA})/I(3350 \text{ \AA})$  with  $\text{N}_2$  pressure in the range 0–100 torr, followed by a more gradual increase at higher pressures and saturation above 500 torr. This behavior of the intensity ratio, which has been reported by other authors<sup>12,13,36</sup> and has also been observed qualitatively in the course of this study, indicates the more likely initial formation of  $^3\text{I}_u$  molecules. If  $^3\text{O}_u^-$  molecules were the first to be formed in three-body collisions involving excited Hg atoms, the above intensity ratio would decrease monotonically with increasing  $\text{N}_2$  pressure and reach a limiting value at pressures above 500 torr.

\*Research supported by the National Research Council of Canada.

†Present address: J.I.L.A., University of Colorado, Boulder, Colo.

‡On leave from the College of Engineering, Bydgoszcz, Poland.

<sup>1</sup>For a review of the early work see, for example, W. Finkelnburg, *Kontinuerliche Spectren* (Springer, Berlin, 1938); P. Pringsheim, *Fluorescence and Phosphorescence* (Interscience, New York, 1949).

<sup>2</sup>F. S. Phillips, Proc. R. Soc. Lond. **A89**, 39 (1913).

<sup>3</sup>Lord Rayleigh, Proc. R. Soc. Lond. **A114**, 620 (1927).

<sup>4</sup>Lord Rayleigh, Proc. R. Soc. Lond. **A137**, 101 (1932).

<sup>5</sup>J. Franck and W. Grotrian, Z. Phys. **4**, 89 (1921).

<sup>6</sup>S. Mrozowski, Z. Phys. **104**, 228 (1937); Z. Phys. **106**, 458 (1937); Z. Phys. **106**, 458 (1937).

<sup>7</sup>S. Mrozowski, Rev. Mod. Phys. **16**, 160 (1944).

<sup>8</sup>A. O. McCoubrey, Phys. Rev. **93**, 1249 (1954).

<sup>9</sup>P. Pringsheim, *Fluorescence and Phosphorescence* (Interscience, New York, 1949).

<sup>10</sup>J. Pitre, K. Hammond, and L. Krause, Phys. Rev. A **6**, 2101 (1972).

<sup>11</sup>J. A. Berberet and K. C. Clark, Phys. Rev. **100**, 506 (1955).

<sup>12</sup>S. Penzes, H. E. Gunning, and O. P. Strausz, J. Chem. Phys. **47**, 4869 (1967).

<sup>13</sup>J. E. McAluff, D. D. Drysdale, and D. J. LeRoy, Can. J. Chem. **46**, 199 (1968).

<sup>14</sup>M. Stupavsky, G. W. F. Drake, and L. Krause, Phys. Lett. A **39**, 349 (1972).

<sup>15</sup>A. C. Vikis and D. J. LeRoy, Phys. Lett. A **44**, 325 (1973).

<sup>16</sup>A. O. McCoubrey and C. G. Matland, Phys. Rev. **92**, 637 (1953).

<sup>17</sup>R. J. Carbone and M. M. Litvak, J. Appl. Phys. **39**, 2413 (1968).

<sup>18</sup>D. C. Lorents, R. M. Hill, and D. J. Eckstrom, Stanford Research Institute Report No. 1, 1972 (unpublished).

<sup>19</sup>A. Corney and G. W. Series, Proc. Phys. Soc. Lond. **83**, 207 (1964).

<sup>20</sup>P. C. Rogers, FRANTIC, program for analysis of exponential growth and decay curves M.I.T. Laboratory of Nuclear Sciences Technical Report No. 76, 1962 (unpublished).

<sup>21</sup>J. S. Deech and W. E. Baylis, Can. J. Phys. **49**, 90 (1971).

<sup>22</sup>T. Holstein, D. Alpert, and A. O. McCoubrey, Phys. Rev. **85**, 985 (1952).

<sup>23</sup>P. B. Sackett, Appl. Opt. **11**, 2181 (1972).

<sup>24</sup>I. Mrozowska, Acta. Phys. Pol. **2**, 81 (1933).

<sup>25</sup>G. Herzberg, *Spectra of Diatomic Molecules* (Van Nostrand, New York, 1950).

<sup>26</sup>R. Lennuier and Y. Crenn, C. R. Acad. Sci. (Paris) **216**, 486 (1943).

<sup>27</sup>T. Holstein, Phys. Rev. **72**, 1212 (1947).

<sup>28</sup>C. G. Matland, Phys. Rev. **92**, 637 (1953).

<sup>29</sup>See Table XIX in A. C. G. Mitchell and M. W. Zemansky, *Resonance Radiation and Excited Atoms* (Cambridge U.P., Cambridge, England, 1971).

<sup>30</sup>M. C. Bigeon, J. Phys. Radium **28**, 51 (1967); J. Phys. Radium **28**, 157 (1967).

<sup>31</sup>J. S. Deech, J. Pitre, and L. Krause, Can. J. Phys. **49**, 1976 (1971).

<sup>32</sup>J. P. Barrat, D. Casalta, J. L. Cojan, and J. Hamel,

- J. Phys. Radium 27, 608 (1966).
- <sup>33</sup>A. B. Callear and G. J. Williams, Trans. Faraday Soc. 60, 2158 (1964).
- <sup>34</sup>J. E. McAlduff and D. J. LeRoy, Can. J. Chem. 43, 2279 (1965).
- <sup>35</sup>J. M. Campbell, S. Penzes, H. S. Sandhu, and O. P. Strausz, Int. J. Chem. Kinet. 3, 175 (1971).
- <sup>36</sup>M. Stupavsky, Ph.D. thesis (University of Windsor, 1971) (unpublished).